Lasers in Manufacturing Conference 2023

3D microstructuring in metals using a UV laser microspot scanning system

Rose Mary [a], Stefan Remund[a], Beat Neuenschwander[a,*]

[a]*Institute for Applied Laser, Photonics and Surface Technologies ALPS, Bern University of Applied Sciences, Pestalozzistrasse 20, CH-3400 Burgdorf, Switzerland*

Abstract

High resolution UV laser micro-ablation and micro-drilling is investigated using a 10 ps, 355 nm ultrashort pulsed laser and a galvanometer scanner equipped with a microscan objective MSE-G2-UV. The microscan extension enables the laser beam to be very tightly focused down to a diameter of < 1.5 µm and thus converts a standard laser scanning system into a microspot scanning system. Laser ablation characteristics in steel, copper and monocrystalline silicon is reported for a repetition rate of 200 kHz. The usually observed cone-like protrusions in steel at higher peak fluences was found to be absent using the microscan. Micro-structuring of various designs that elucidate the resolutions achievable with such a small spot is also presented. Micro-drilling in Mylar film with an exit hole diameter of ~3 µm is also reported.

Keywords: laser micromachining; uv laser ablation; microscan; micro-ablation; micro-drilling

1. Introduction

Ultrafast laser ablation is a well-established field with a wide application range by virtue of its minimal heat-affected zone, flexible processing capability, excellent precision, and superior quality [1]. The technology is also continuously advancing due to the development of novel processing techniques as well as new products in the market, making ongoing research crucial for harnessing its full potential.

For laser machining of micro-structures that has feature sizes of the order of a few micrometers, single pulse laser ablation using a small spot is the most direct approach. With the finest possible resolution

* Corresponding author. Tel.: +41 34 426 42 20; fax: +41 34 423 15 13.
E-mail address: beat.neuenschwander@bfh.ch

defined by the optical diffraction limit (~λ/2), shifting the operating wavelength to UV is beneficial. The use of ultra-high-resolution scan-optics provides the second step to reducing the feature size. In this paper, we report the experimental studies of UV laser ablation using a microscan objective MSE-G2, which provides a focal spot diameter of <1.5 µm and a corresponding Rayleigh range of ~5 µm. Termed as a '1 µm laser knife', the objective transforms the setup into a microspot scanning system. Basic laser ablation characteristics of steel, copper, and monocrystalline silicon are investigated. The microspot scanning system is used to ablate various interesting structures that gives a visualization of the resolution possible with the system. Micro-drilling in mylar film is also discussed.

2. Experimental Setup

Figure 1 shows the schematic of the experimental setup used for the studies. A 10 ps FUEGO laser from Lumentum, set to its third harmonic wavelength of 355 nm was used. The linearly polarized laser beam was first expanded using an appropriate telescope to a diameter of 6 mm and then converted into circular polarization using a λ/4 wave plate. The beam was then guided using folding mirrors to the scanner optics which consisted of an intelliSCANde14 scanner from Scanlab and the microscan MSE-G2-UV objective from Pulsar Photonics. The microscan objective is equipped with a coaxial camera which helps in the positioning of the samples in the focal plane of the laser. The microscan has a scan field of 500 x 500 µm^2.

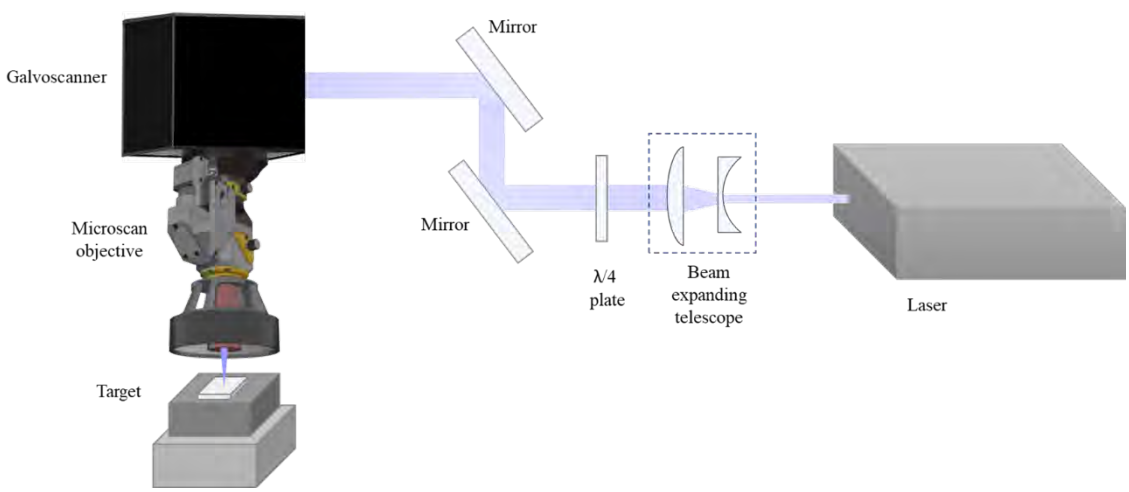

Fig. 1. Schematic of the experimental setup for laser ablation using the microscan objective

The ablation characteristics in the UV were investigated at a fixed laser repetition rate of 200 kHz for stainless steel 1.4301/AISI 304, copper DHP and monocrystalline silicon <100>. Square cavities with a side length of 200 µm and 10 overscans were ablated, with a spot overlap of 75%. High accuracy ablation by line scanning is achieved by synchronizing the galvo scanner and the laser pulse train [2-3]. Following laser ablation, the samples were cleaned in an ultrasonic bath with isopropanol. The sample analysis, namely, the depth and structural profiles were measured using a GBS smart white light interferometer and a scanning electron microscope (SEM).

3. Laser ablation

For laser ablation using a Gaussian beam, the specific removal rate (the removed volume per average power) as a function of applied peak fluence ϕ_0 is given by the expression,

$$\frac{dV}{dE} = \frac{dV}{dt \cdot P_{av}} = \frac{1}{2} \cdot \frac{\delta}{\phi_0} \cdot \ln^2\left(\frac{\phi_0}{\phi_{th}}\right) \tag{1}$$

where, δ is the energy penetration depth, ϕ_{th} is the threshold fluence and $\phi_0 = \frac{2E_p}{\pi\omega_0^2}$ is the peak fluence in the center of the beam. This model assumes the ablation depth to be within the Rayleigh range of the focusing objective. The highest specific removal rate obtained at the optimum fluence $\phi_{0,opt}$ is given by

$$\left.\frac{dV}{dE}\right|_{\max} = \frac{2}{e^2} \cdot \frac{\delta}{\phi_{th}}; \quad \phi_{0,opt} = e^2 \cdot \phi_{th} \tag{2}$$

The threshold fluence and penetration depth for laser ablation is found to depend on the spot size and the pulse duration of the beam [4].

3.1. Steel

[5,6] reports the occurrence of a bumpy surface quality in steel 1.4301/AISI 304 for laser ablation in the IR, with the effect attributed to heat accumulation effects at high peak fluences. For investigations in the UV, the laser ablation characteristics using the microscan objective was compared with that using a standard galvoscanner with a 100 mm f-theta objective. The specific removal rate of steel 1.4301 with the conventional system, comprising of the galvoscanner and the f-theta lens (Linos AG) is shown in Fig. 2(a). A 350 fs Satsuma laser (from Amplitude) working at 343 nm and 500 kHz was used for this experiment. The focused laser beam measured a spot size of $\omega_0 = 5\mu m$. For laser ablation in the IR, the measured energy specific volume was found to deviate from the model fit given in Equation 1. In UV however, the model fits the measured values very well. Despite this, an onset of cavitation [7,8] is still observed at higher peak fluences (at already twice the optimum peak fluence), as shown in the SEM image in Fig. 2(b).

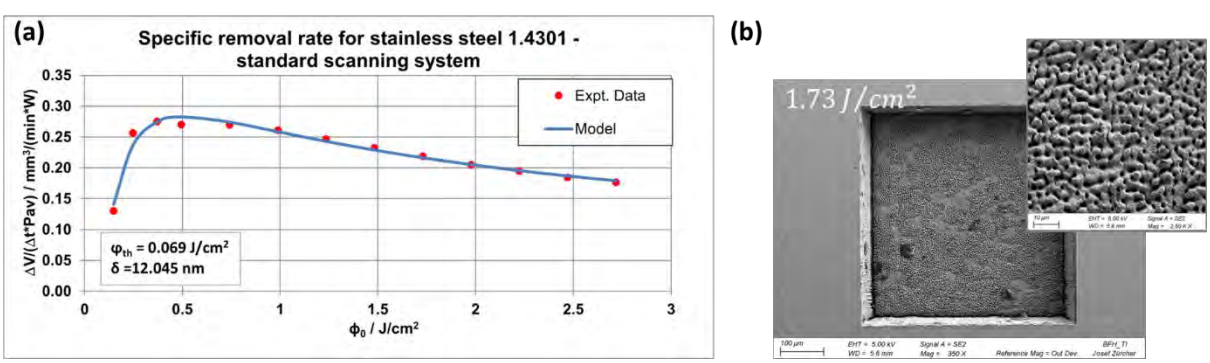

Fig. 2. (a) Specific removal rate of steel as a function of peak fluence at 343 nm using a galvanometer scanner and a standard 100 mm f-theta objective; (b) SEM image of square cavity ablated at a peak fluence of 1.73 J/cm^2. Cavitation effects can be observed, with a higher magnification SEM image shown as inset.

The specific removal rate for steel at 200 kHz using the microspot scanning system is shown in Fig. 3. The model fit (blue solid line) according to (1) is found to deviate at higher fluence values. However, no cavitation with the bumpy surface structure is observed at these fluences. The deviation in the model can be attributed to the ablated depth exceeding the Rayleigh range (~ $5\mu m$) within the first couple of overscans. By compensating for the beam spot size along the ablated depth according to $\omega(z) = w_0\sqrt{1+(z/z_R)^2}$, a modified fit model (red dashed line) can be calculated which fits the measured values well. Both the models were found to yield similar values for the threshold laser fluence and the penetration depth. A surface roughness of < 200 nm is measured for laser ablation at the optimal peak fluence of 3.7 J/cm^2. Fig. 3(b) shows the SEM image of a square cavity ablated at a peak fluence of thrice the optimum fluence value.

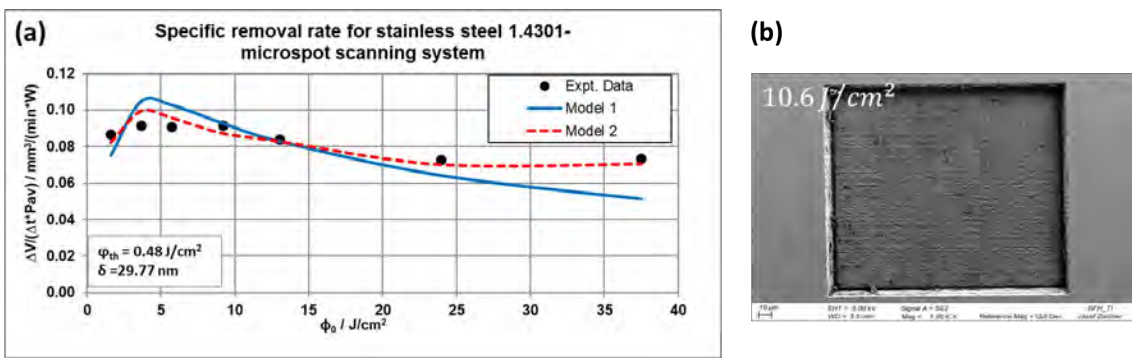

Fig. 3. (a) Specific removal rate of steel using the microspot scanning system; (b) SEM image of the ablated surface at a peak fluence of three times that of the optimum value. There is no onset of bumpy surface features using the microscan.

3.2. *Copper*

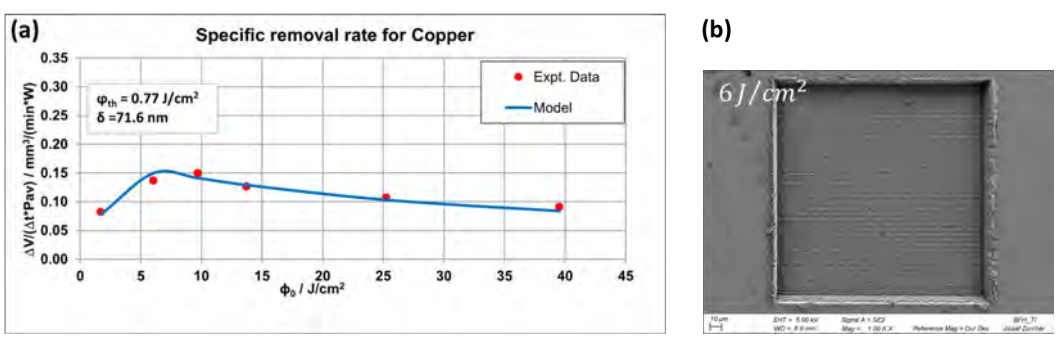

Fig. 4. (a) Specific removal rate of copper at 200 kHz laser repetition rate using the microscan objective; (b) The SEM image of the smooth ablated surface near the optimum peak fluence.

Fig. 4(a) shows the specific removal rate for Copper DHP as a function of peak fluence for laser ablation using the microspot scanning system. The experimental data and the model fit were found to be in good agreement. The threshold fluence and the energy penetration depth for copper is higher than that for steel, at 0.77 J/cm^2 and 71.6 nm, respectively. Fig. 4(b) shows the SEM image of the smooth ablated surface at a pulse fluence of 6 J/cm^2 with a corresponding surface roughness of 120 nm.

3.3. Silicon

Fig. 5 (a) shows the SEM images of square cavities ablated in <100> monocrystalline silicon at pulse fluences of 5.2, 12.7 and 40 J/cm^2 with corresponding surface roughness values of 0.5, 1 and 6 µm, respectively. With increasing peak fluences, the surface roughness values are also found to increase, as shown in Fig. 5(b). The ablated material is also found to be redeposited at high peak fluences.

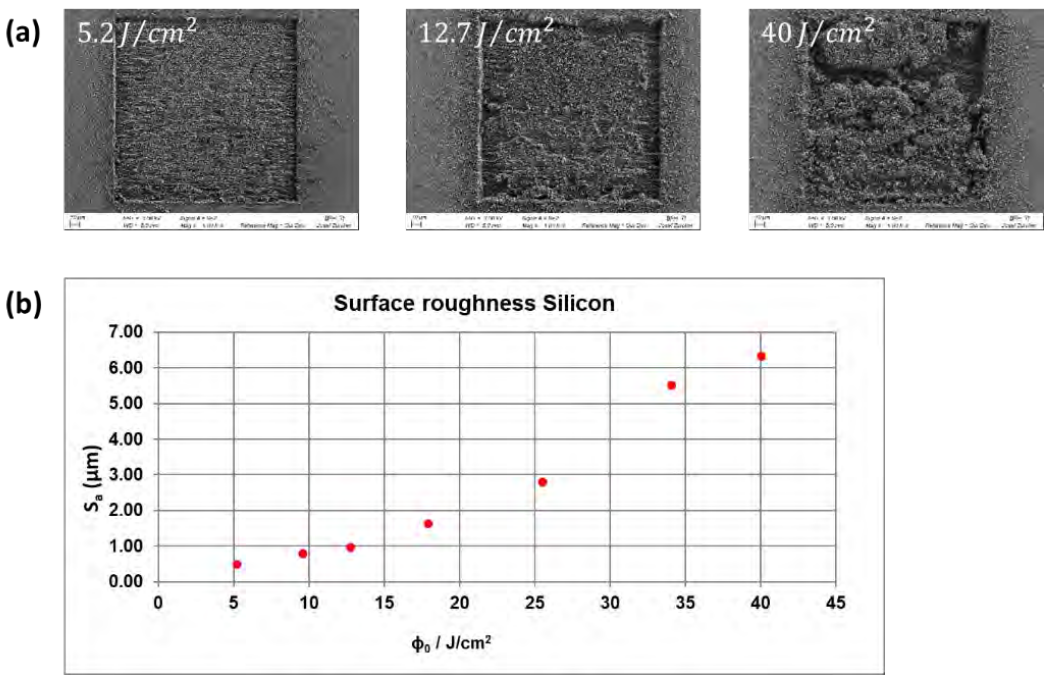

Fig. 5. (a) SEM images of square cavities ablated in Silicon using the microscan objective at different laser peak fluences'; (b) The surface roughness in silicon as a function of laser peak fluence.

3.4. Micro-structures in Steel and Copper

The resolution of the structures achievable with the microspot scanning system was explored by ablating a variety of patterns; the exemplars of which are shown in Fig. 6. Fig. 6(a) is the topography of Switzerland, machined onto steel with 36 overscans at 40 mW average power, a peak fluence of 4.4 J/cm^2 and a repetition rate of 1 MHz. Fig. 6(b) is a pair of Globe images in copper with each globe spanning just over 300 µm in diameter. This was ablated using 10 overscans and an average power of 44 mW.

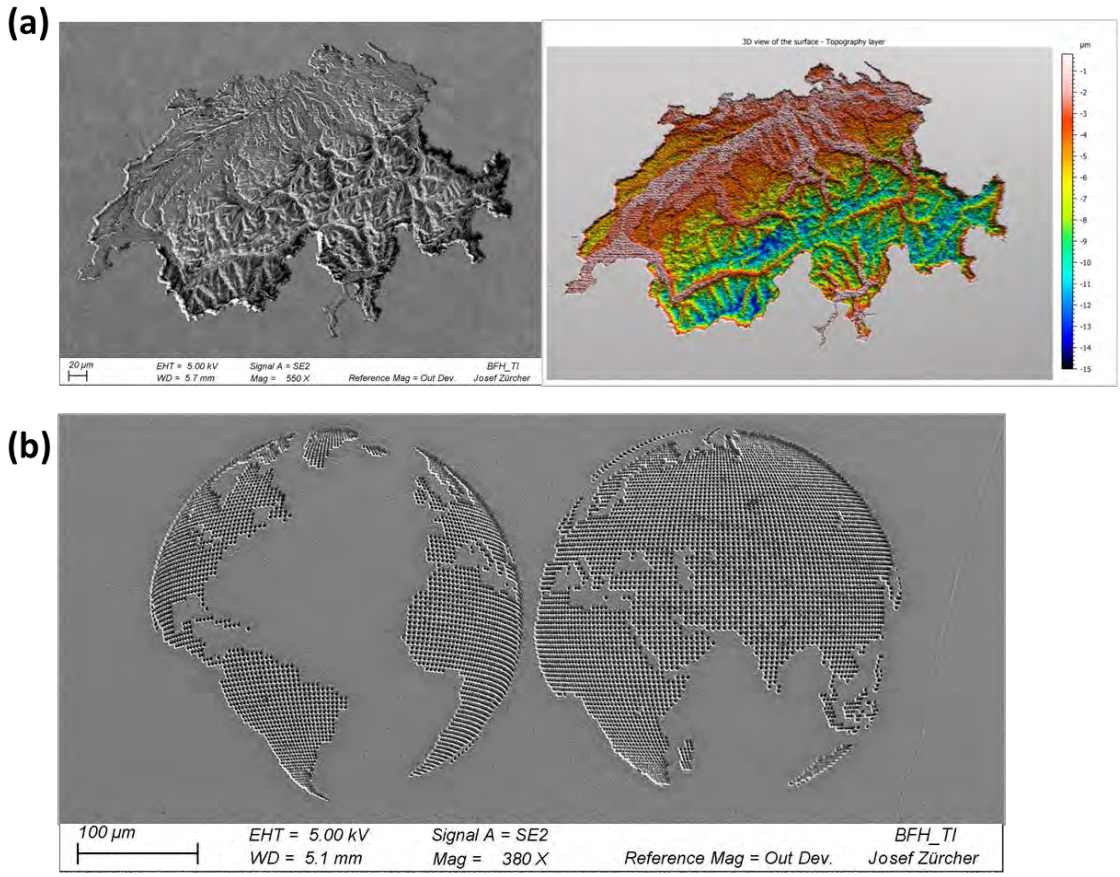

Fig. 6. (a) The topographic map of Switzerland ablated in steel. The SEM image is on the left and the depth distribution map measured using a white light interferometer is on the right. The structure has a dimension of 495 µm x 335 µm; (b) The SEM image of a pair of Globes ablated in copper.

4. Micro-drilling in Mylar film

Micro-drilling using the microspot scanning system in a 20 µm thick mylar film was also investigated using the same line scanning strategy. Squares with pixel dimensions in decremental steps – 10, 5, 2 and 1 pixel^2 were ablated at 200 kHz repetition rate; its resolution defined by the diameter of the focused laser spot. Fig. 7 (a,b) shows the exit hole dimensions for the 5 and 2 pixel^2 micro-holes ablated with a laser peak fluence of 50 J/cm^{2}and 20 overscans. The 5 px^2 hole was drilled through with an exit hole diameter measuring ~3 µm. The 2 px^2 hole was not drilled all the way through.

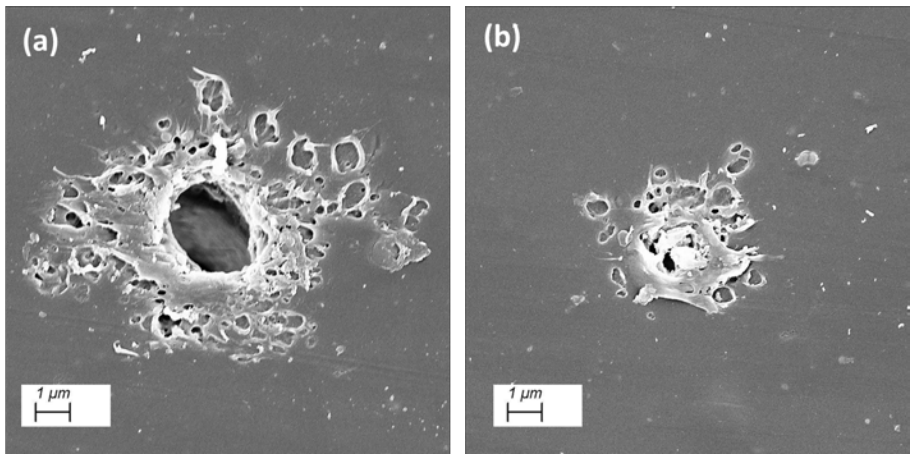

Fig 7. SEM images of exit hole diameters of (a) 5 pixel^2 and (b) 2 pixel^2 wide micro-holes in mylar

The complexity in drilling holes of a few pulse-wide can be attributed to several reasons, including shielding effects from the plasma and Fresnel reflections at the steep side walls of the drilled hole. These can lead to a drop in the peak fluence to below the ablation threshold and thus not reach the rear exit of the hole [9]. Reducing the repetition rate of the laser is one way to reduce the shielding and beam perturbation effects associated with the drilling of small holes. Fig. 8 shows a micro-stencil drilled in Mylar using the microspot scanning system at 50 J/cm^{2}and 4 overscans.

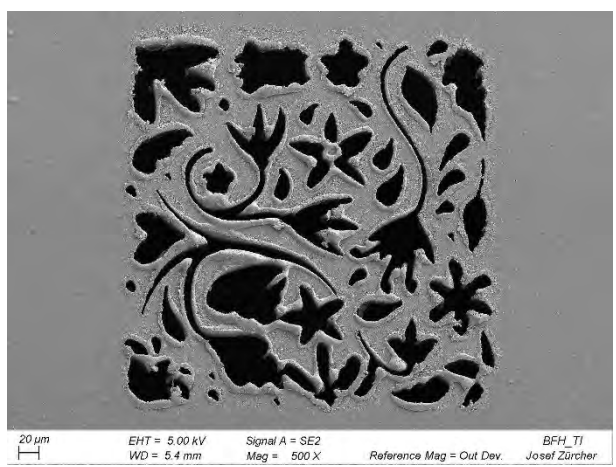

Fig. 8. SEM image of a micro-stencil ablated in a 20 µm thick Mylar film using the microscan objective.

5. Conclusion

Micro-ablation characteristics in steel, copper and silicon <100> were investigated using a UV microspot scanning system. In the case of steel, the measured specific removal rate was found to deviate from the model fit, but without the appearance of any cone-like protrusions typical at high peak fluences. The deduced threshold fluence and energy penetration depth was also higher than that observed for conventional laser-galvoscanner systems with larger beam waists. Unlike the smooth ablation properties in

steel and copper, laser ablation in <100> silicon was found to be dominated by heat accumulation, resulting even in the re-deposition of the ablated volume. The resolution and precision possible by the microscan objective were demonstrated by ablating various structures in steel and copper. Experiments in micro-drilling in Mylar was also demonstrated with an observed exit hole diameter of the order of twice the laser beam waist.

Acknowledgements

Thanks to Josef Zürcher, Berner Fachhochschule-TI, for all the scanning electron microscope measurements.

References

[1] Sugioka, K., 2017 “Progress in ultrafast laser processing and future prospects,” Nanophotonics, vol. 6, p. 393.
[2] B. Jaeggi, B. Neuenschwander, M. Zimmermann, M. Zecherle, and E. W. Boeckler, 2016 “Time-optimized laser micro machining by using a new high dynamic and high precision galvo scanner,” in Proc. SPIE 9735, Laser Applications in Microelectronic and Optoelectronic Manufacturing (LAMOM) XXI, p. 973513.
[3] B. Jaeggi, B. Neuenschwander, U. Hunziker, et al., 2012 “Ultra-high precision surface structuring by synchronizing a galvo scanner with an ultra-short-pulsed laser system in MOPA arrangement,” in Laser Applications in Microelectronic and Optoelectronic Manufacturing (LAMOM) XVII, p. 82430K.
[4] Michalina Chaja, Thorsten Kramer, Beat Neuenschwander, 2018 “Influence of laser spot size and shape on ablation efficiency using ultrashort pulse laser system”, Procedia CIRP, 74, p. 300
[5] B. Jaeggi, R. Stefan, R. Streubel, B. Gökce, S. Barcikowski, B. Neuenschwander, 2017 “Laser Micromachining of Metals with Ultra-Short Pulses: Factors Limiting the Scale-Up Process”, Journal of Laser Micro Nanoengineering. 12. p. 267.
[6] M. Gafner, S. Remund, M. Chaja, B. Neuenschwander, 2021 “High-rate laser processing with ultrashort laser pulses by combination of diffractive elements with synchronized galvo scanning”, Advanced Optical Technologies,10, no. 4–5, p. 333.
[7] B. Neuenschwander, T. Kramer, B. Lauer, and B. Jaeggi, 2015 “Burst mode with ps- and fs-pulses: influence on the removal rate, surface quality, and heat accumulation,” in Proc. SPIE 9350, Laser Applications in Microelectronic and Optoelectronic Manufacturing (LAMOM) XX, vol. 9350, p. 93500U.
[8] M. Tsukamoto, T. Kayahara, H. Nakano, et al., 2007 “Microstructures formation on titanium plate by femtosecond laser ablation,” J. Phys. Conf. Ser., vol. 59, p. 666–669.
[9] Feuer, A., Weber, R., Feuer, R. et al. 2021 “High-quality percussion drilling with ultrashort laser pulses.” Appl. Phys. A 127, p. 665.